Available online at www.sciencedirect.com
SCIENCE DIRECT
Journal of Molecular Structure 790 (2006) 152–159
Journal of MOLECULAR STRUCTURE
www.elsevier.com/locate/molstruc

Temperature dependent deuterium quadrupole coupling constants of short hydrogen bonds

Xingang Zhao, Paolo Rossi [1], Valeri Barsegov [2], Jun Zhou, Jeffrey N. Woodford [3], Gerard S. Harbison *

Department of Chemistry, University of Nebraska at Lincoln, 508 Hamilton Hall, Lincoln, NE 68588-0304, USA

Received 1 September 2005; received in revised form 31 October 2005; accepted 31 October 2005
Available online 25 January 2006

Abstract

Very short hydrogen bonds universally show large positive dependences of the deuterium NMR quadrupolar coupling constant with temperature. We present temperature dependent NMR data for eight such systems, with O···O distances of between 238 and 250 pm, and show we can model the temperature dependences by density functional methods, as long as proper attention is paid to intermolecular effects and intermode couplings.

Keywords: Hydrogen bonds; NMR; Deuterium quadrupole

1. Introduction

The hydrogen bond, or 'hydrogen bridge', as it was originally known, seems to have been independently conceived twice within a single year at the University of California at Berkeley, by Maurice Huggins, in an undergraduate thesis, and by Latimer and Rosebush [1]. Shortly thereafter, Bragg [2] proposed that a network of these bonds could explain the tetrahedral arrangement of oxygen atoms in water ice. Huggins, who seems to be the unacknowledged father of the hydrogen bond, also first proposed another seminal idea [3]: that if the distance between the two oxygens in an ice-like hydrogen bond (which we will denote, in the notation first proposed by Huggins [4], as O–H···O) becomes short enough, the 'central hump' in the potential for displacement of the hydrogen parallel to the hydrogen bond direction will disappear, and there will be a single energy minimum, in the center. Thus, was born the idea of the experimentally elusive single-minimum hydrogen bond.

Huggins, using a primitive Morse potential, estimated the 'hump' would disappear at $r_{OO} \sim 265$ pm. Speakman [5], in his early X-ray crystallographic characterization of potassium hydrogen bis-phenylacetate, the seminal member of the hydrogen dicarboxylate class of strong hydrogen bonds, observed that the twin oxygens of the O–H···O system were symmetrically displaced about a crystallographic center, approximately 255 pm distant, and astutely noted that this could be explained either by a Huggins-type single minimum potential, or by disordered hydrogens with 50% occupancy in a double potential minimum. While the structures of many significantly shorter O–H···O systems have since been determined, we can seldom if ever unequivocally distinguish between Speakman's two alternatives, even by neutron crystallography; hydrogen bonds with r_{OO} distances as short as 239 pm [6] often yield centered, anisotropic thermal ellipsoids, which could in principle be consistent either with a single, highly anisotropic single well potential, or a low-barrier double well. Thus, nearly 70 years since Huggins first sketched a set of double-well potentials merging into single wells as r_{OO} decreases, the question of how short the O···O distance has to be to create a true single well potential is still a controversial one.

Since structural methods have been surprisingly impotent regarding this issue, spectroscopy has instead come to the force. Any survey of the early work in the field must note

* Corresponding author. Tel.: +1 402 472 9346; fax: +1 402 472 9402.
E-mail address: gerry@setanta.unl.edu (G.S. Harbison).
[1] Present address: Center for Advanced Biotechnology and Medicine, 679 Hoes Lane Piscataway, Piscataway NJ 08854-5638, USA.
[2] Present address: Institute for Physical Science and Technology. University of Maryland, College Park, MD 20742, USA.
[3] Department of Chemistry and Biochemistry, Eastern Oregon University, La Grande, OR 97850, USA.

0022-2860/$ - see front matter © 2006 Published by Elsevier B.V.
doi:10.1016/j.molstruc.2005.10.053

the observation of the vibrational 0–1 transition of a symmetric O–H···O system, by Hadzöi in 1961; the observation of infrared absorbtions between 120 and 150 cm^{-1} in potassium dihydrogenphosphate and isomorphs, phenylphosphinic acid, and potassium hydrogen bis-4-nitrobenzoate clearly showed these systems to be low-barrier double-wells, with frequencies considerably higher than conventional tunneling frequencies of 'normal' hydrogen bonds, but far lower than would be expected for a hydrogen in a single minimum. Where direct observation of infrared transitions has been difficult or impossible, inelastic neutron scattering has often served as a substitute.

It is clear that measurement of a full set of vibrational transitions allows an exact delineation of the potential surface; in fact, given the constraints on the possible vibrational potentials for a hydrogen bond, even a single correctly-assigned 0–1 vibrational frequency gives an excellent indication of the height of the barrier, although interpretation is made more difficult by mode-coupling, particularly with the soft and strongly coupled O···O mode. The rub is, of course, the measurement and assignment of this vibrational spectrum may not be straightforward.

Other spectroscopic measurables, therefore, have instead been sought. NMR provides several possibilities. It has been known for many years that, both in solution [7], by multiple pulse solid-state NMR [8], and most recently by high-speed magic-angle spinning ^1H NMR [9] that the chemical shift of the O–H···O proton depends strongly on the hydrogen bond strength, ranging from less than 10 ppm for weakly hydrogen bonded systems to over 20 for the strongest hydrogen bonds. Qualitative agreement with this trend was obtained in ab initio calculations [10].

The deuterium quadrupole coupling constant, which we will denote by eqV_{zz}, which is directly proportional to the electric field gradient at the nuclear site, and can therefore simply be calculated from the electronic ground state electron density, similarly has a strong monotonic dependence on hydrogen bond strength. Berglund and Vaughan in 1980 [8] compiled 27 quadrupole coupling constants over a range of r_{OO} values from 243.7 pm to effectively infinity (the isolated O–H group in calcium hydroxide); their data show that eqV_{zz} decreases from approximately 275 kHz at infinite r_{OO} to around 50 kHz for the shortest hydrogen bonds. Unfortunately, ab initio calculations based on the equilibrium structure, even with high-level corrections for electron correlation, do not accurately reproduce the experimental data; this has greatly hindered theoretical interpretation, but has made analysis of correlations [8,11] between experimental measurables all the more important.

The failure so far to quantitatively interpret NMR data means that while we can use chemical shifts and deuteron coupling constants to obtain relative strengths of hydrogen bonds, we cannot yet use their magnitudes to gauge the form of the potential. Three years ago [12], therefore, we proposed that the temperature dependence of the deuterium quadrupole coupling constant might be more informative than its absolute magnitude. We noted that two compounds with very strong hydrogen bonds—sodium deuterium bis-4-nitrophenolate dihydrate [13] and the enolized tautomer of 4-cyano-2,2,6,6-tetramethyl-3,5-heptanedione show large anomalous temperature coefficients; in both cases, the deuterium electric quadrupole coupling constant increases with temperature—whereas the commonly encountered thermal averaging mechanisms tend cause eqV_{zz} to decrease with temperature. Miyakubo and Nakamura [14] and previously Kalsbeek et al. [15] had reported similar phenomena for other strongly hydrogen bonded deuterons. We proposed that the root of the phenomenon required two conditions to be fulfilled; a vibrational first excited state with a much larger eqV_{zz} than the ground state, and a first vibrational frequency in the range 100–700 cm^{-1}, making the first excited state thermally accessible around and below room temperature. We have since reported similar large positive temperature coefficients for the deuteron eqV_{zz} and the proton chemical shift in the strongly O–H···N system 4-methylpyridine pentachlorophenolate; the group of Lluch had previously proposed [16] that temperature dependent proton chemical shifts might be a diagnostic feature of low-barrier hydrogen bonds. In the present work, we report a survey of quadrupole coupling constants in 10 strongly hydrogen bonded compounds, and advance a quantitative explanation for the observed temperature coefficients.

2. Theory

Electronic structure calculations were carried out using the program GAMESS, using a 6-311G**(3df, 3pd) basis set, with the B3LYP density functional, integrated over a $128\times32\times16$ grid, and using a polarizable continuum model for the dielectric with $\varepsilon=\varepsilon_\infty=5.0$ and a nominal solvent radius of 200 pm. The hydroxyl hydrate structure (H–O–H···$^-$O–H) was used as a model, as in previous work [12]. After optimization of the structure in C_{2h} symmetry, energies and electric field gradients were calculated over a 41×41 grid of points spaced by 40 pm about median values of $r_{OO}=245.3$ pm and r_H (hydrogen displacement from the center of the system)$=0$. The energies were fit to a full polynomial of order 6 in r_{OO} multiplied by an even polynomial of order 10 in r_H; this fit gave a maximum residual of less than 0.2 mHartree. The two-dimensional linear Schrödinger equation was then solved variationally, using a basis set of 36 two-dimensional harmonic oscillator wavefunctions, with independent variational optimization of the harmonic oscillator force constants. Energies and wavefunctions were computed for the ground state and the first excited states along the r_H and r_{OO} coordinates, the expectation value of the electric field gradient tensor computed for each of these states, a Boltzmann-weighted average performed, and then the EFG tensor diagonalized, with the quadrupole coupling constant calculated as previously described [12].

3. Methods

3.1. Sample preparation

Detailed preparative methods for the deuterated derivatives are as follows. Nitromalonamide (**I**) was prepared by nitration of malonamide with fuming red nitric acid by the classic procedure of Ratz [17] and recrystallized from

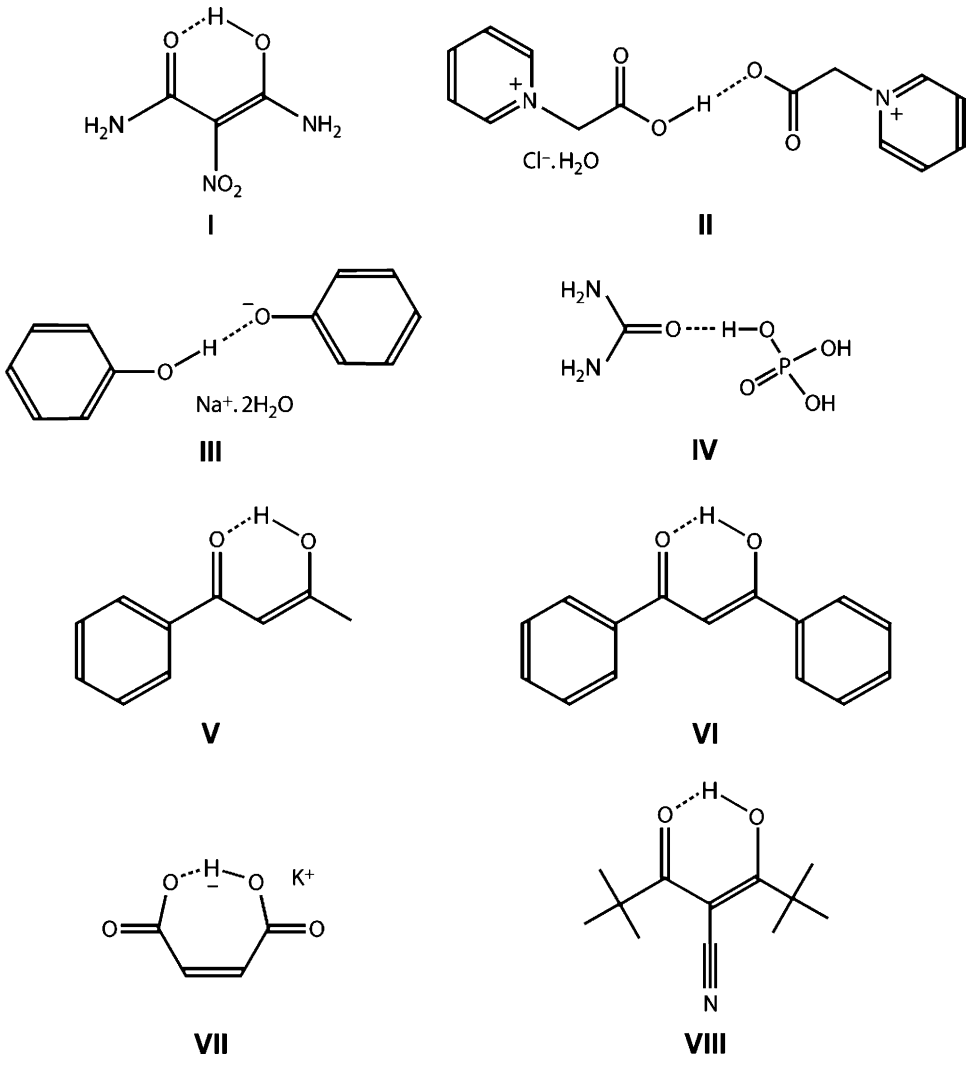

Fig. 1. Structures of compounds studied in this work.

methoxyethanol. To synthesize nitromalonamide-d_5, the undeuterated material was dissolved in dimethylsulfone, and precipitated by addition of D_2O; the powder was about 95% deuterated by NMR. Bis(pyridinebetaine) hydrochloride monohydrate (**II**) was prepared by adding chloroacetic acid to pyridine and stirring overnight at room temperature [18]. The white crystals were collected and dissolved in methanol. By adding diethylether dropwise, **II** was precipitated. **II**-d_3 was made by exchanging **II** with an excess of CH_3OD. Urea phosphate-d_7 (**III**) was obtained by combining equimolar quantities of orthophosphoric acid and urea in D_2O, and allowing the material to crystallize by slow evaporation. Sodium deuterium bis-4-nitrophenolate dideuterate (**IV**-d_5) was obtained from a saturated solution containing a 2:1 molar ratio of 4-nitrophenol and sodium hydroxide in D_2O. After crystallization, it was dried in vacuo and transferred to a sealed tube for NMR measurements. Benzoylacetone (**V**) and dibenzoylmethane (**VI**) were purchased from Aldrich, and crystallized from C_2H_5OD solution to yield **V**-d_1 and **VI**-d_1. Potassium hydrogen maleate (**VII**) was made by neutralizing a suspension of maleic acid in water with 1 equiv. of potassium hydroxide, and crystallizing from alcohol/water. The product was recrystallized from C_2H_5OD/D_2O to give **VII**-d_1.

The structures of compounds **I–VII** are shown in Fig. 1.

3.2. NMR

Deuterium spectra of **IV**-d_5 were acquired at 46.77011 MHz with a home-built spectrometer and probe, over a 213–333 K temperature range, using a standard solid echo pulse sequence, with a $\pi/2$ pulse of 2 μs and inter-pulse delays of 50 μs. At each temperature, two spectra were collected; one with a short relaxation delay (typically 50 ms–5 s, depending on temperature); and a second with a long delay (typically 60 s). Simulations of the deuteron powder spectra, shown below the experimental spectra, were carried out using the MXQET program. Spectra of **V**-d_1 and **VI**-d_1 were obtained on the same instrument, with a 3 μs $\pi/2$ pulse and an interpulse delay τ of 80 μs.

The singularities in the spectra were extracted by inspection, and the quadrupole coupling constant and asymmetry parameter η obtained using standard formulas. Spin lattice

relaxation times T_1, were determined by a three parameter fit to data from an inversion recovery quadrupole echo pulse sequence. Because these relaxation times were often very long (see below) recovery delays of 200 s were used between transients.

Variable temperature ^{1}H and ^{2}H NMR MAS spectra for compounds **I**, **II** and **III** were obtained on a Bruker Avance NMR spectrometer operating at 14 T, using a simple one-pulse sequence. $\pi/2$ pulses were 4 μs for proton and 3 μs for deuterons, respectively. Both isotopes were referenced to the isotropic frequencies of residual protons and of deuterons in solid dimethylsulfone-d_6, whose chemical shift was assumed to lie 2.4 ppm downfield from TMS. MAS sideband intensities were fit to computed patterns using eqV_{zz} and η as adjustable parameters, using a computer program based on the formulas derived by Herzfeld and Berger [19].

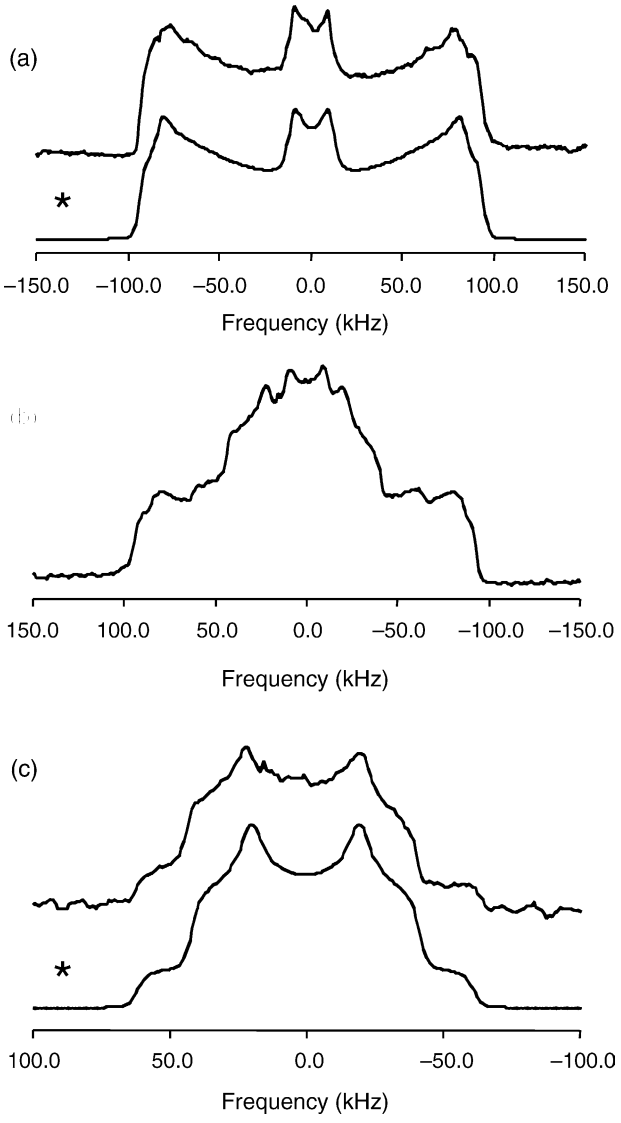

Fig. 2. ^{1}H NMR spectra of sodium deuterium bis-4-nitrophenolate dideuterate, obtained (a) with a short recycle delay of 50 ms (b) a long recycle delay of 60 s (c) difference. Simulations (asterisked) are shown under the experimental spectra.

4. Results

Spectra of **IV**-d_5, obtained at 273 K as described above, with relaxation delays of 50 ms and 60 s are shown in Fig. 2(a) and (b), respectively. Because the phenolic deuteron had a long relaxation time, roughly independent of temperature, the spectra obtained at short relaxation times contained only signals from the four water deuterons (Fig. 2(a)), while the long-relaxation delay spectra had contributions from both water and phenolic deuterons (Fig. 2(b)); subtraction of the two spectra gave spectra from the phenolic deuterons alone (Fig. 2(c)). The value of the quadrupole coupling constant and asymmetry parameter obtained are consistent with the MAS sideband patterns previously measured by Wolf et al. [20] (those authors did not extract quantitative quadrupolar coupling parameters from their spectra).

Room temperature static quadrupole-echo ^{2}H spectra of benzoylacetone-d_1 (**V**-d_1) and dibenzoylmethane-d_1 (**VI**-d_1) are shown in Fig. 3(a) and (b), respectively; both these and Fig. 2(c) are typical of the large-η deuterium Pake doublets obtained from strongly hydrogen-bonded deuterons.

Fig. 4 shows ^{1}H and ^{2}H 14 T MAS spectra of the residual protons and the deuterons of nitromalonamide-d_5 (**I**-d_5). The proton spectrum shows one sharp peak around 18.5 ppm, which we assign to the O–H···O proton, and two complex multiplets between 7 and 11 ppm which are assigned to the four amide protons. A signal around 2.5 ppm arises from residual DMSO. Fine structure in the amide doublets arises from the slight non-degeneracy of the shifts, and also from the residual dipolar interaction between ^{1}H and the quadrupolar ^{14}N nucleus, which

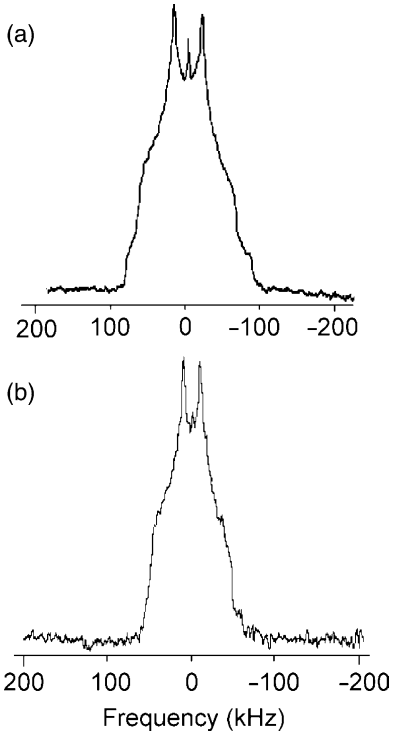

Fig. 3. ^{2}H solid-state NMR spectra of (a) benzoylacetone-d_1 (b) dibenzoylmethane-d_1.

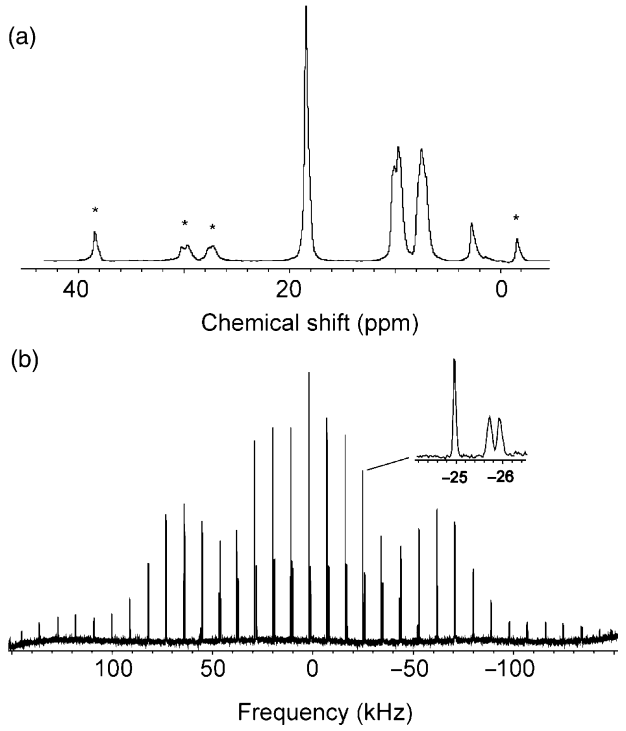

Fig. 4. ^{1}H MAS solid-state NMR spectrum of nitromalonamide-d_5 (**I**) (b) ^{2}H MAS solid-state NMR spectrum of nitromalonamide-d_5, showing in the inset the chemical shift resolution of the centerband.

is not fully removed by MAS. The deuterium spectrum (Fig. 3(b)) is somewhat more poorly resolved, but the O–D···O proton and the two amide peaks are clearly visible (inset), and therefore full MAS sideband patterns can be determined for each; these allow reconstruction of the deuterium eqV_{zz} and η.

Fig. 5 shows the ^{2}H 14 T MAS spectra of the deuterons of bis(pyridinebetaine) hydrochloride monohydrate-d_3 (**II**-d_3). In this relatively simple spectrum only two sets of MAS sideband patterns are resolved, from the O–D···O and the water of hydration respectively. The D_2O signal has the $\eta = 1$ sideband envelope characteristic of a flipping water molecule; the considerable asymmetry of the O–D···O sideband envelope is indicative of a large chemical shielding anisotropy.

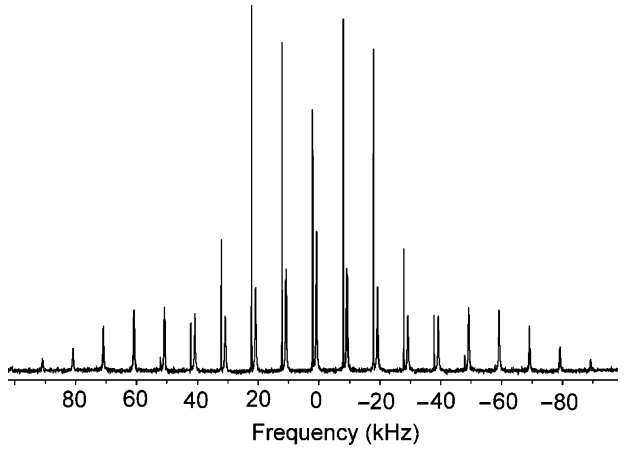

Fig. 5. ^{2}H MAS solid-state NMR spectrum of bis(pyridinebetaine) hydrochloride monohydrate (**II**).

Fig. 6 shows ^{1}H and ^{2}H 14 T MAS spectra of the residual protons and the deuterons of urea phosphoric acid-d_7 (**III**-d_7). The proton spectrum shows the expected sharp peak around 21 ppm for the O–H···O proton, a pair of resonances between 13 and 15 ppm arising from the other two P–O–H protons, and two complex multiplets between 8 and 12 ppm which are assigned to the four amide protons. The signal around 4.7 ppm arises from the liquid HDO contaminant; magic-angle spinning rotational sidebands are asterisked. The deuterium spectrum (Fig. 5(b)) is more cluttered than the comparable spectrum of **I**-d_5, but the O–D···O signal is still clearly resolved (inset).

In every case, quadrupole coupling constants were extracted either from the singularities of the static patterns, or by fitting the sideband envelopes; these are plotted as a function of temperature in Fig. 7, along with previously [6] obtained data for 3-cyano-2,4-pentanedione-d_1 (**VIII**-d_1). The temperature dependences were fit to quadratic functions, and the first derivative of the dependence of the quadrupole coupling constant with temperature at 250 K extracted; these temperature derivatives are compiled, along with the extracted

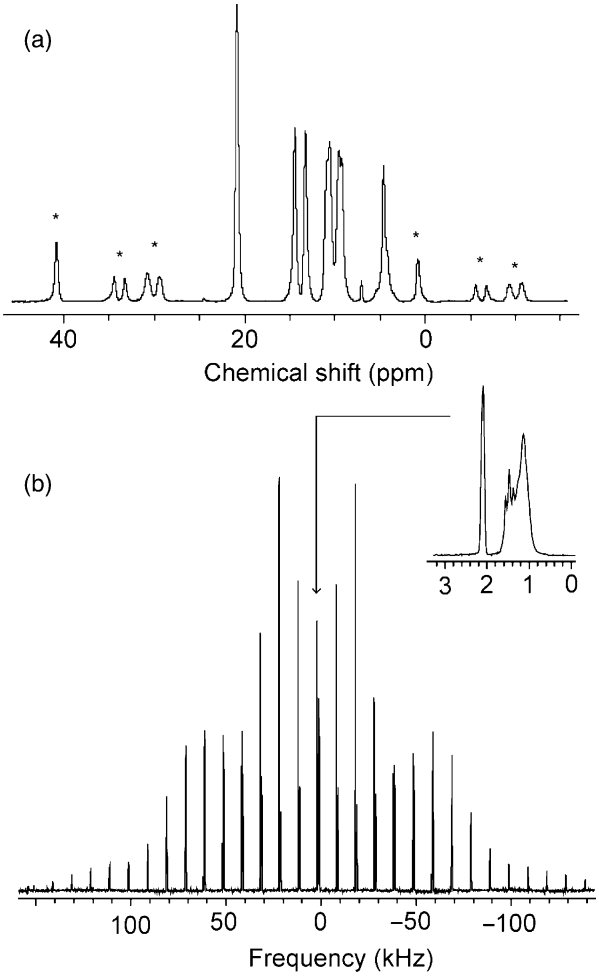

Fig. 6. (a) ^{1}H MAS solid-state NMR spectrum of urea phosphoric acid-d_7 (**III**) (b) ^{2}H MAS solid-state NMR spectrum of (**III**)-d_7. (Inset) chemical shift resolution of the centerband.

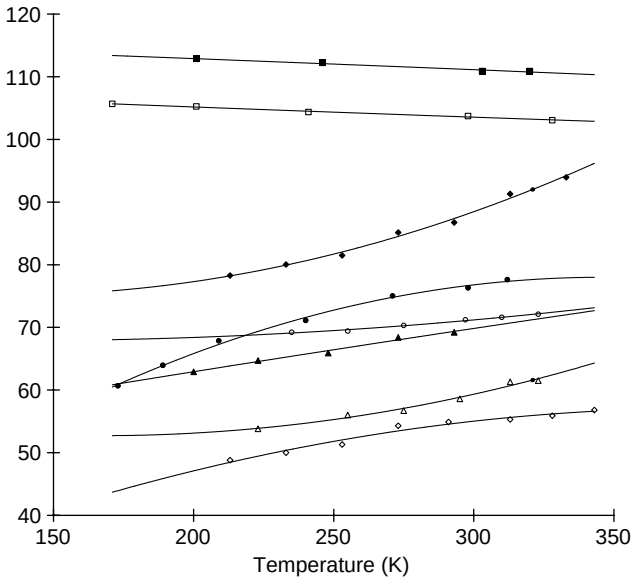

Fig. 7. Temperature dependence of the deuterium quadrupole coupling constants of (filled box) **V**; (open box) **VI**; (filled diamond) **IV**; (filled circle) **VIII**; (open circle) **III**; (filled circle) **VII**; (filled triangle) **I**; (open triangle) **II**; (filled diamond) **VII**.

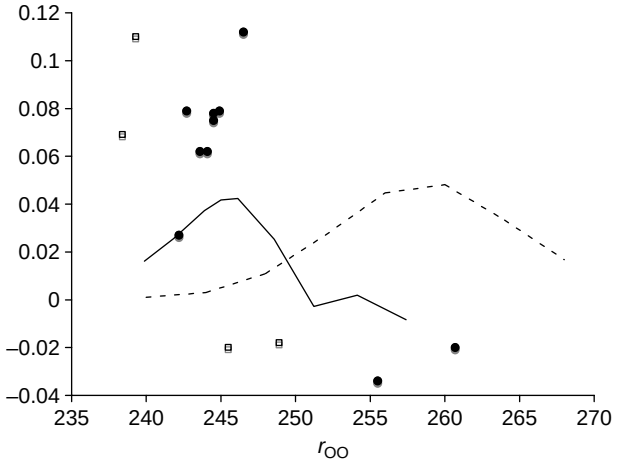

Fig. 8. Experimental temperature coefficients of the deuterium quadrupole coupling constant, at 250 K of systems with (filled circles) linear hydrogen bonds; (open boxes) non linear hydrogen bonds, compared with (dashed line) uncoupled vacuum calculations; (solid line) coupled calculations with a continuum dielectric constant of 5.

deuterium quadrupole coupling constants and proton chemical shifts, where available, in Table 2 and plotted in Fig. 8 versus the O···O distance, given in Table 1 with the relevant reference, along with some values obtained from the literature. In this plot, we chose to separate systems where the hydrogen bond forms part of a six-membered ring, where the hydrogen bond is substantially non-linear, from those where the hydrogen bond is linear or nearly linear.

5. Discussion

The experimental temperature coefficients presented in Fig. 8 contend persuasively to be diagnostic of short strong hydrogen bonds. Clearly, such large, counter-intuitive coefficients indicate a thermally accessible vibrational excited state with a larger eqV_{zz} than the ground state. While the unsophisticated model we presented previously [12] provides a plausible qualitative explanation for the temperature coefficients, it is clear from the computed values of the coefficients, shown as a hatched line in Fig. 8, that the simple one-dimensional potential does not quantitatively reproduce experimental data. Having examine a plethora of possible explanations for this discrepancy (use of Gaussian rather than Slater type orbitals, insufficient attention to electron correlation, interactions with lattice vibrations) we settled on two primary sources. One is neglect of the dielectric: symmetrical hydrogen bonds are necessarily non-polar along the hydrogen bond axis, while displacement of the hydrogen to either side creates a component of the molecular dipole along this axis. Such a dipole interacts with a polarizable medium, lowering the energy and thus relatively stabilizing off-center hydrogens. While these effects are more significant in other systems (particularly where displacement of the hydrogen creates a zwitterion), even in symmetric systems they tend to deepen double-well potentials.

A more significant effect still is the coupling between the hydrogen displacement mode and the longitudinal hydrogen bond O···O mode itself. The latter, in effect, creates the potential in which the hydrogen atoms vibrate. It is typically highly anharmonic and of higher symmetry than the hydrogen atom displacement, and therefore couples with both the vibrational ground and excited states of the hydrogen displacement mode. Because of the anharmonicity, the first excited vibrational state of ψ_{OO} necessarily has an effective

Table 1
Crystal structure data for compounds used in this work

Molecule	Label	r_{OO} (pm)	r_{OH} (pm)	$r_{H\cdots O}$ (pm)	T (K)	Ref.
Nitromalonamide	I	239.1	114.0	130.8	15	[21]
Bis(pyridine betaine) hydrochloride monohydrate	II	243.6	–	–	300	[22]
Urea phosphate	III	242.2	115.8	126.7	15	[23]
Sodium hydrogen bis-4-nitrophenolate dihydrate	IV	246.5	123.2	123.2	20	[24]
Benzoylacetone	V	249.9	124.5	132.9	20	[25]
Dibenzoylmethane	VI	245–246	–	–		[26,27]
Potassium hydrogen maleate	VII	242.7	121.5	121.5	5	[28]
4-Cyano-2,2,6,6-tetramethyl-3,5-heptanedione	VIII	239.3	121.6	122.0	20	[6]

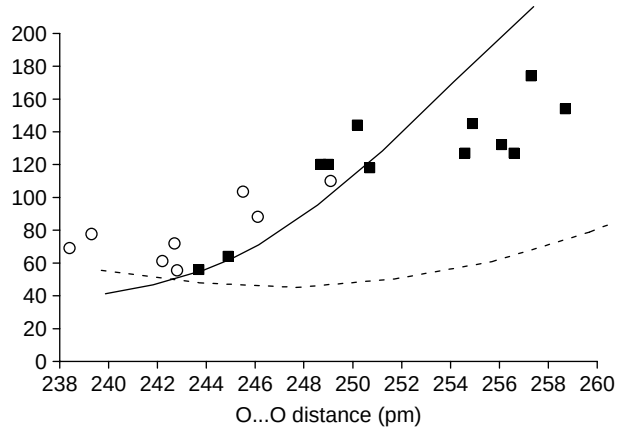

Fig. 9. Experimental ^{2}H NMR quadrupole coupling constants at 300 K from (filled boxes) the work of Berglund and Vaughan; (open circles) the present work, compared with (dashed line) uncoupled vacuum calculations; (solid line) coupled calculations with a continuum dielectric constant of 5.

average r_{OO} value significantly larger than the ground state, and therefore has a lower energy. Coupling of these modes together, therefore, lowers the first vibrational excited state energy, thus reducing the vibrational splitting and making the first vibrational state more thermally accessible. The effect is twofold; first, the maximum temperature coefficient is shifted to shorter r_{OO} distances; and second, the ground and particularly the first excited state quadrupole coupling constant acquire increased contributions from instantaneous configurations with larger r_{OO} values, thence increasing the thermal equilibrium value of eqV_{zz}. The effect on the temperature coefficient is dramatically illustrated in Fig. 8, where the solid line depicts $d(eqV_{zz})/dT$, computed assuming a reasonable solid-state dielectric and coupling between the two aforementioned modes. The computed curve now matches the maximum value of r_{OO} almost exactly, albeit the temperature coefficients are still approximately a factor of 2 smaller. As can be seen in Fig. 9, we also get a grossly improved agreement between the absolute magnitude of eqV_{zz} and experimental data. The points in Fig. 9 correspond to experimental values of eqV_{zz} tabulated by Berglund and Vaughan [8], supplemented with our values for compounds **I**–**VIII**. The lines are computed from the one-dimensional vacuum calculations (hatched) and the two-dimensional coupled, polarizable continuum model (solid). Clearly, the latter model agrees far better with the data, particularly considering the experimental data contain a considerable diversity of O–H···O systems, and asymmetrical as well as symmetrical hydrogen bonds (Table 2).

The major remaining discrepancy between experiment and theory lies in the magnitude of the experimental temperature coefficients. The origin of this discrepancy is likely our failure to include the effects of thermal expansion of the r_{OO} distance itself. Since thermal expansion of intermolecularly hydrogen-bonded crystals often leads to a significant increase in r_{OO}, and since the quadrupole coupling constant depends strongly on r_{OO}, we expect that this effect will augment the effect of thermal excitation of the vibrationally exited states top increase the positive dependence of eqV_{zz} on temperature. Preliminary calculations on **IV**, where the r_{OO} dependence on temperature has been measured crystallographically, seem to support this conjecture.

The four non-linear hydrogen bonds studied fall on a slightly different curve, and maximum temperature coefficients are obtained for somewhat smaller r_{OO} distances. It is likely that this is simply due to the non-linear nature of the minimum of the potential along the O···O direction; we have not yet completed calculations for such systems.

The significant interaction between O···O and O–H modes in these systems to some extent invalidates the discussion of what constitutes a 'low-barrier hydrogen bond', since the hydrogen wavefunction is no longer considered to be moving in a one-dimensional potential. It is better, perhaps, to look at the shape of the wavefunction itself. We find that $|\psi_H|^2$ has

Table 2
Measured temperature derivative of the quadrupole coupling constant with temperature at 250 K, from this work and others

Compound	r_{OO} (pm)	$d(eqV_{zz})/dT$ (kHz/K)	eqV_{zz} kHz, 300 K	δ_{OH} ppm, 300 K	^{1}H NMR, Ref.	^{2}H NMR, Ref.
Urea phosphate (**III**)	242.2	0.027	71	20.9	This work	This work
Potassium hydrogen maleate (**VII**)	242.7	0.079	55	21.0	[29]	This work
Bis(pyridine betaine) hydrochloride monohydrate (**II**)	243.6	0.062	59	–		This work
Potassium hydrogen succinate	244.1	0.062	53	–		[15]
Methylammonium hydrogen succinate monohydrate	244.5	0.075	59	–		[15]
KH acetylene-dicarboxylate	244.5	0.078	60.5	–		[14]
RbH acetylene-dicarboxylate	244.9	0.079	66	–		[14]
Sodium hydrogen bis-4-nitrophenolate dihydrate (**IV**)	246.5	0.112	87	–		This work
Sodium hydrogen malonate	255.5	−0.034	165.5	–		[15]
$KHCO_3$	260.7	−0.02	154.5	–		[14]
Nitromalonamide (**I**)	238.4	0.069	69	18.5	This work	This work
4-Cyano-2,2,6,6-tetramethyl-3,5-heptanedione (**VIII**)	239.3	0.110	77	19.0	[6]	This work
Dibenzoylmethane (**VI**)	245.5	−0.020	104	18.1	[9]	This work
Benzoylacetone (**V**)	248.9	−0.018	111	16.2	[9]	This work

Linear systems are given above non-linear systems.

a single maximum below 245 pm and a double maximum above this value, and thus for r_{OO} values under 245 pm linear O–H···O systems are best described by a model of a centered proton rather than a proton equally distributed between two wells. These systems still have significant deuterium temperature coefficients, albeit below the maximum observed.

In conclusion, with proper consideration of the medium dielectric and of the coupling between coupled hydrogen bond modes, we can get good agreement between computed and experimental NMR temperature coefficients, and these coefficients are both on theoretical and experimental grounds believed to be diagnostic of hydrogen bonds which are transitional between low-barrier double well and true single well systems.

Acknowledgements

The importance of the coupling between O···O and O–H modes was pointed out to the authors by Bruce Hudson of Syracuse University. GSH is grateful for research support from the National Institutes of Health (R01 GM 065252).

References

[1] W.M. Latimer, W.H. Rodebush, J. Am. Chem. Soc. 42 (1920) 1419.
[2] W.H. Bragg, Proc. Phys. Soc. 34 (1922) 98.
[3] M.L. Huggins, J. Phys. Chem. 40 (1936) 723.
[4] R.G. Bhat, R. Gudihal, Curr. Sci. 85 (2003) 839.
[5] J.C. Speakman, J. Chem. Soc (1949).
[6] J.A. Belot, J. Clark, J.A. Cowan, G.S. Harbison, A.I. Kolesnikov, Y.-S. Kye, A.J. Schultz, C. Silvernail, X. Zhao, J. Phys. Chem. B 108 (2004) 6922.
[7] L.W. Reeves, E.A. Allan, K.O. Strømmme, Can. J. Chem. 38 (1960) 1249.
[8] B. Berglund, R.W. Vaughan, J. Chem. Phys. 73 (1980) 2037.
[9] Th. Emmler, S. Gieschler, H.H. Limbach, G. Buntkowsky, J. Mol. Struct. 470 (2004) 29.
[10] R. Ditchfield, J. Chem. Phys. 65 (1976) 3123.
[11] H.-H. Limbach, M. Pietrzak, S. Sharif, P.M. Tolstoy, I.G. Shenderovich, S.N. Smirnov, N.S. Golubev, G.S. Denisov, Chem. Eur. J. 10 (2004) 5195.
[12] X. Zhao, M. Dvorak, C. Silvernail, J.A. Belot, G.S. Harbison, Solid State NMR 22 (2002) 363.
[13] P. Rossi, PhD Thesis, University of Nebraska, 2001.
[14] K. Miyakubo, N. Nakamura, Z. Naturforsch. 57a (2002) 337.
[15] N. Kalsbeek, K. Schaumburg, S. Larsen, J. Mol. Struct. 299 (1993) 155.
[16] M. Garcia-Viloca, R. Gelabert, À. González-Lafont, M. Moreno, J.M. Lluch, J. Am. Chem. Soc. 120 (1997) 10203.
[17] F. Ratz, Monatsh. Chem. 25 (1904) 55.
[18] J.T. Esdall, J. Wyman Jr., J. Am. Chem. Soc. 57 (1964) 1935.
[19] J. Herzfeld, A.E. Berger, J. Chem. Phys. 73 (1980) 6021.
[20] C.A. Klug, P.L. Lee, L.-S.H. Lee, M.M. Kreevoy, R. Yaris, J. Schaefer, J. Phys. Chem. 101 (1997) 8086.
[21] G.K.H. Madsen, C. Wilson, T.M. Nymand, G.J. McIntyre, F.K. Larsen, J. Phys. Chem. A 103 (1999) 8684.
[22] X.M. Chen, T.C.W. Mak, J. Mol. Struct. 221 (1990) 265.
[23] C.C. Wilson, Acta Crystallogr. B57 (2001) 435.
[24] S.S. Marimanikkuppam, I.-S.H. Lee, D.A. Binder, V.G. Young, M.M. Kreevoy, Croat. Chem. Acta 69 (1996) 1661.
[25] B. Schiøtt, B.B. Iversen, G. Kent, H. Madsen, T.C. Bruice, J. Am. Chem. Soc. 120 (1998) 12117.
[26] F.J. Hollander, D.H. Templeton, A. Zalkin, Acta Crystallogr. B29 (1973) 1552.
[27] M.C. Etter, D.A. Jahn, Z. Urbanczyk-Lipkowska, Acta Crystallogr. C43 (1987) 260.
[28] F. Fillaux, N. Leygue, J. Tomkinson, A. Cousson, W. Paulus, Chem. Phys. 244 (1999) 387.
[29] A.M. Achlama, U. Kohlschütter, U. Haeberlen, Chem. Phys. 7 (1975) 287.